ELSEVIER

International Journal of Mass Spectrometry 185/186/187 (1999) 25–35

International Journal of Mass Spectrometry

On the formation of the carbon dioxide anion radical $CO_2^{-\cdot}$ in the gas phase

Detlef Schröder*, Christoph A. Schalley, Jeremy N. Harvey, Helmut Schwarz*

Institut für Organische Chemie, Technische Universität Berlin, D-10623 Berlin, Germany

Received 8 April 1998; accepted 5 May 1998

Abstract

Although carbon dioxide is well known to have a negative electron affinity, the $CO_2^{-\cdot}$ anion radical can be generated in several types of mass spectrometric experiments, such as collisional activation of carboxylate ions or double electron transfer to $CO_2^{+\cdot}$. In particular, it is shown that vibrational excitation of the precursor cations increases the yield of the bound anion radicals in charge inversion experiments. Combined application of experimental and theoretical means indicates that for bent geometries, the $^2A_1$ state of the carbon dioxide anion radical is stable against electron detachment in the μs timescale of the experiments. In a chemical sense, the $CO_2^{-\cdot}$ anion radical can be regarded as an activated carbon dioxide unit in which the C–O bonds are weakened and the carbon center exhibits distinct radical character. Thus, $CO_2^{-\cdot}$ constitutes a new type of distonic anion in which the charge and the unpaired electron are located in different symmetry planes. (Int J Mass Spectrom 185/186/187 (1999) 25–35) © 1999 Elsevier Science B.V.

Keywords: Carbon dioxide; Anion radicals; Mass spectrometry; Ab initio calculations; Distonic anions

1. Introduction

The activation of carbon dioxide represents a considerable challenge in contemporary chemistry [1], not to mention the molecule's probable role in global warming. A fundamental difficulty in activating carbon dioxide arises from its inertness caused by the lack of a dipole moment in conjunction with a huge thermochemical stability. One potential route to achieve an activation of the molecule involves initial electron transfer to carbon dioxide to yield the corresponding anion radical $CO_2^{-\cdot}$ as an intermediate. Recently, experimental evidence for the occurrence of electron transfer in cobalt complexes of carbon dioxide has been presented [2].

In the gas phase, however, solitary carbon dioxide exhibits a negative electron affinity, and thus electron loss according to reaction (1) is exothermic by about 10–15 kcal/mol [3].

$$CO_2^{-\cdot} \rightarrow CO_2 + e^- \quad (1)$$

Despite this thermochemical argument, the carbon dioxide anion radical as well as $(CO_2)_n^{-\cdot}$ clusters have been observed in several spectroscopic experiments [4]. Further, the solvated $CO_2^{-\cdot}$ anion radical has been observed both in the gas phase as well as in condensed matter [3,5–7], and these species are well character-

* Corresponding authors.

Dedicated, with admiration, to M.T. Bowers on the occasion of his 60th birthday.

PII S1387-3806(98)14042-3

ized by EPR spectroscopy [8]. Compton et al. have estimated a maximal lifetime of about 90 μs for the $CO_2^{-\cdot}$ anion radical [3]. Bowen and Eaton were able to record photoelectron spectra of several $(CO_2)_n^{-\cdot}$ clusters including $n = 1$ [7]. Another experimental indication for a finite lifetime of $CO_2^{-\cdot}$ was provided by the observation of the isotopic exchange reaction (2) in flow-tube studies. These have demonstrated that the degenerate oxygen-atom exchange via reaction (2) can compete with the highly exothermic associative electron detachment according to reaction (3) [9,10].

$$^{12}C^{16}O + {}^{18}O^{-\cdot} \rightarrow {}^{12}C^{18}O + {}^{16}O^{-\cdot} \quad (2)$$

$$^{12}C^{16}O + {}^{18}O^{-\cdot} \rightarrow {}^{12}C^{16}O^{18}O + e^- \quad (3)$$

The formation of the anion radical of carbon dioxide has also been observed in high-energy collisions of anions such as carboxylates and related species [11–14], in the fragmentation of some carboxylates at low energies [15,16], as well as in the dissociation of $[CO_2]_n^{-\cdot}$ cluster ions [4]. Finally, the $CO_2^{-\cdot}$ anion radical has formed the subject of a number of theoretical investigations [17–21].

2. Experimental and computational details

The experiments were carried out using a VG-ZAB-2HF/AMD604 four-sector mass spectrometer of BEBE configuration (B stands for magnetic and E for electric sectors), which has been described elsewhere [22,23]. Direct electron or chemical ionization of carbon dioxide did not yield a significant signal for $CO_2^{-\cdot}$. Instead, the anion radical was made by either (i) collisional activation of mass-selected carboxylate ions or (ii) by charge inversion of $CO_2^{+\cdot}$ using xenon as a collision gas. So-formed $CO_2^{-\cdot}$ was mass selected with the subsequent sectors of the tandem mass spectrometer in order to study the lifetime of the anion radical. MS/MS experiments with $CO_2^{-\cdot}$, such as charge reversal of the anion to the cation [24], were however impossible due to the low ion current of $CO_2^{-\cdot}$ in conjunction with the high ionization energy (IE) of neutral CO_2 (13.8 eV) and of its possible fragments, i.e. IE(O) = 13.6 eV, IE(CO) = 14.0 eV [25]. Carboxylate ions were made by chemical ionization of the corresponding acid with water or dinitrogen oxide as reagent gases. The cation radical of carbon dioxide was made by ionization of the neutral either by electron ionization (EI, electron energy 100 eV, repeller voltage ca. 20 V) or self-chemical ionization (CI, electron energy 100 eV, repeller voltage ca. 0 V) using CO_2 as a reagent gas. The ions of interest, having 8 keV kinetic energy, were mass-selected using either $B(1)$ only or $B(1)/E(1)$ at mass resolutions of $m/\Delta m = 2000$–4000. The energy balance of the charge reversal process (ΔE_{CR}) was determined for $B(1)$ mass-selected cations which were collided with xenon in the field-free region preceding $E(1)$ and the anions were recorded with $E(1)$ at an energy resolution of $E/\Delta E = 7000$. The energy demand was derived from the high energy onsets of the parent ion and of the charge reversed signals using the onset for the process $O_2^{+\cdot} + 2\ Xe \rightarrow O_2^{-\cdot} + 2\ Xe^{+\cdot}$ with $\Delta E_{CR} = 2\ IE(Xe) - IE(O_2) - EA(O_2) = 2 \cdot 12.13\ eV - 12.07\ eV - 0.45\ eV = 11.74\ eV$ as a reference for the calibration of the energy scale [25–28]. Most of the spectra were accumulated and on-line processed with the AMD/Intectra data system, and 10 to 30 spectra were averaged to improve the signal-to-noise ratio. Due to hardware limitations, the measurements of the energy deficits were, however, recorded as single scans using an x/y recorder, and the data given were derived from the average of several independent experiments.

Quantum chemical calculations were carried out using the BECKE3LYP method implemented in the GAUSSIAN94 program package [29]. Additional calculations have been performed using the coupled cluster approach including single and double excitation with a perturbative estimate of the triple excitation, CCSD(T) [30], using the MOLPRO94 suite of programs [31]. Vertical electron affinities (EA_v) or detachment energies (DE_v) of the neutrals and anions, respectively, were calculated as total energy differences between the anions and neutrals at the equilibrium geometries of the corresponding species. In the BECKE3LYP calculations, the standard 6-311++G(d,p) basis sets have been applied for oxygen and carbon, while for CCSD(T) we employed the much larger

aug-cc-pVTZ basis sets [32,33]. The geometries of the neutral, anionic, and cationic species were optimized at the BECKE3LYP level, and the analytical force constants were derived at the same level in order to characterize the stationary points as minima or transition structures, respectively, and to account for zero-point vibrational energy (ZPVE) as well. The geometry of the point of lowest energy where the anionic and neutral surfaces cross, i.e. the minimum energy crossing point (MECP) [34–36], was optimized also at the BECKE3LYP level using a recently developed method which combines the energies and analytical energy gradients computed for the two surfaces to yield two "effective" gradients which lead to the MECP [37]. The geometry and energy of the MECP were reoptimized at the CCSD(*T*)//BECKE3LYP level, using the hybrid method of reference [37] with CCSD(*T*) energies and BECKE3LYP gradients.

3. Results

In the diluted gas phase, anion radicals of the elemental composition $[C,O_2]^{-\cdot}$ can be formed by two different routes. (i) Collisional activation of carboxylate ions and some of their derivatives leads to weak yet clearly detectable signals at $m/z = 44$ according to reaction (4) with R = H, CH_2, and CH_3) [11,12]. For some carboxylates in which R represents a stable radical having a negative electron affinity, e.g. $R = i - C_3H_7$, the $[C,O_2]^{-\cdot}$ fragment gives rise to a major signal in the CA mass spectrum [13]. (ii) It will be shown further below that collisional double electron transfer with projectiles having kinetic energies in the keV regime can be used to invert the charge of the cation radical of carbon dioxide into an anion radical according to reaction (5).

$$R{-}COO^- \rightarrow R^{\cdot} + [C,O_2]^{-\cdot} \quad (4)$$

$$CO_2^{+\cdot} + 2e^- \rightarrow [C,O_2]^{-\cdot} \quad (5)$$

The fact that $[C,O_2]^{-\cdot}$ generated in reactions (4) and (5) can be observed in a standard mass-spectrometric setup operating with keV ions implies that the anion radicals formed must live long enough to be transmitted through the analyzers (μs time scale). However, these findings contrast the well-established fact that carbon dioxide has a negative electron affinity [3]. Thus, several questions arise from the experimental observation of a signal corresponding to $[C,O_2]^{-\cdot}$. At first, it has to be ensured that the signals observed are not due to impurities giving rise to isobaric interferences. Next, other isomers than the anion radical of carbon dioxide may be formed in high-energy collisions and these may indeed exhibit positive electron affinities with respect to the corresponding neutrals (see below). Finally, the mechanism for the formation of $[C,O_2]^{-\cdot}$ needs to be analyzed in order to understand the nature of the associated processes. The latter aspect is particularly intriguing with regard to the reason why the negative charge is located at the $[C,O_2]$ moiety rather than at the radical $R^{\cdot}$ lost in reaction (4). To answer these questions, we have performed a combined experimental and theoretical study of the $[C,O_2]^{+/0/-}$ system, including an experimental estimate of the lifetime of the anion radical and an examination of the mechanism of formation of the metastable anion radical under the experimental conditions.

3.1. Experimental results

Let us first describe the formation of $[C,O_2]^{-\cdot}$ by loss of a hydrogen atom from formate ion $HCOO^-$. In the collisional activation mass spectrum of $HCOO^-$ with helium used as collision gas, the $[C,O_2]^{-\cdot}$ fragment represents the base peak (100%) along with small amounts of $O^{-\cdot}$ (5%) and HO^- (1%) [11,12,38]. Contribution of isobaric interferences can be ruled out upon careful analysis of the isotope pattern around the $HCOO^-$ precursor ion, further, the CA mass spectrum of $DCOO^-$ is very similar to that of $HCOO^-$, being dominated by the loss of a D atom along with minor amounts of $O^{-\cdot}$ and DO^-.

The generation of a genuine $CO_2^{-\cdot}$ anion radical by homolytic cleavage of the C–H bond in $HCOO^-$ is somewhat unexpected, because thermochemistry predicts preferential formation of the complementary products, i.e. hydride ion H^- concomitant with neutral CO_2, as the least endothermic fragmentation channel (Table 1), but despite careful tuning of the

Table 1
Calculated and experimental reaction enthalpies (kcal/mol) for the fragmentation of formate ion.

	Process	ΔH_R calc.[a]	ΔH_R exp.[b]
Anion fragmentation	$HCOO^- \rightarrow H^- + CO_2$	52.5	51.6
	$HCOO^- \rightarrow HO^- + CO$	56.6[c]	51.8[c]
Dissociative neutralization	$HCOO^- \rightarrow CO_2 + H^{\cdot} + e^-$	72.6	69.0
Electron detachment	$HCOO^- \rightarrow HCOO^{\cdot} + e^-$	79.0	73.3
Anion fragmentation	$HCOO^- \rightarrow CO_2^{-\cdot} + H^{\cdot}$	79.0	—
	$HCOO^- \rightarrow O^{-\cdot} + HCO^{\cdot}$	141.6	147.6
	$HCOO^- \rightarrow HCO^- + O$	169.0	167.1

[a] Energetics calculated with B3LYP/6-311++G(d,p) including ZPVE corrections; data adopted from [11,12].
[b] Experimental values taken from [25].
[c] Formation of HO^- + CO requires ca. 9 kcal/mol in excess of the reaction endothermicity due to the presence of a kinetic barrier in this channel [11,12].

instrument, this channel could not be observed. From a thermochemical point of view, formation of HO^- + CO is also favorable, but it requires a rearrangement of formate ion into the hydroxyacyl structure $HOCO^-$ which is associated with a sizable kinetic barrier [11,12,38]. Accordingly, the HO^- fragment is of minor abundance in the CA spectrum of $HCOO^-$. Electron detachment as well as dissociative neutralization have similar, or even lower energy demands than the formation of $CO_2^{-\cdot}$. Both processes can, however, not be monitored in conventional CA experiments, but their occurrence has recently been demonstrated in a detailed examination of neutral $[C,H,O_2]^{\cdot}$ radicals by mass spectrometric [39,40] and other means [41]. The $O^{-\cdot}$ fragment observed in the CA mass spectrum of $HCOO^-$ is probably due to direct C–O bond rupture and will not be pursued any further.

In summary, the generation of (metastable) $CO_2^{-\cdot}$ by collisional activation of formate ion appears energetically feasible, but the less endothermic fragmentation to yield hydride ion concomitant with neutral CO_2 is expected to compete efficiently. Considering the significantly positive electron affinity of hydrogen atom [EA(H) = 0.78 eV] as compared to the negative electron affinity of carbon dioxide, the observation of a direct fragmentation according to reaction (4) with R = H is indeed somewhat surprising. Further doubt as to the occurrence of a simple C–H bond cleavage is nurtured by the peak shape of the $CO_2^{-\cdot}$ signal. The formation of metastable $CO_2^{-\cdot}$ from formate ion according to reaction (4) with R = H must occur close to the thermochemical threshold, because otherwise $CO_2^{-\cdot}$ is likely to contain excess internal energy and thus bound to undergo electron detachment. Accordingly, the kinetic energy released in reaction (4) should be small for R = H, thus giving rise to a narrow peak for the $CO_2^{-\cdot}$ fragment. Further, also isomerization of formate to $HOCO^-$ prior to fragmentation cannot account for the kinetic energy release, because the associated activation barrier is well below the $CO_2^{-\cdot}$ + $H^{\cdot}$ exit channel [11]. Experimentally, however, a broad peak is observed, and an apparent kinetic energy release of about 200 meV can be derived from the half-heights of the parent and the fragment ion signals. Note, however, that the width of the fragment signal is also due to collisional broadening.

These arguments indicate that processes other than simple collision-induced dissociation may be involved in reaction (4) for R = H. This assumption is further supported by the experimental finding that collisional activation of $HCOO^-$ with xenon as a collision gas leads to a similar fragmentation pattern, i.e. $CO_2^{-\cdot}$ (100%), HO^- (3%), and $O^{-\cdot}$ (15%), respectively, as found for helium, but the overall fragment yield with xenon exceeds that obtained with helium by about a factor of 10. A different situation is encountered upon collisional activation of isobutyrate, i.e. reaction (4) with $R = i\text{-}C_3H_7$ [13]. In this case, formation of $CO_2^{-\cdot}$ is a major process upon collisional activation, and the apparent kinetic energy release in the collisional-activation mass spectrum is much smaller (~100 meV) for the $CO_2^{-\cdot}$ fragment formed from $i\text{-}C_3H_7CO_2^-$. Thus, homolytic cleavage of the α–C–C bond upon collisional activation may well occur in this case (see below).

Charge inversion of the $CO_2^{+\cdot}$ cation radical with xenon as a collision gas (Table 2) also gives rise to a clearly detectable signal for $CO_2^{-\cdot}$, while the base peak in the $^+CR^-$ spectrum corresponds to $O^{-\cdot}$ which is probably formed by dissociative ionization according to reaction (6).

Table 2
Anion signals observed in the $^{+}CR^{-}$ mass spectra (xenon, 80% *T*) of $CO_2^{+\cdot}$ generated by either EI or CI of carbon dioxide (intensities relative to the base peak).

Ionization mode	$CO_2^{-\cdot}$ [a]	$O_2^{-\cdot}$	$O^{-\cdot}$	$C^{-\cdot}$
EI, repeller voltage ~20 V	4	<1	100	<1
CI, repeller voltage ~0 V	1	<1	100	<1

[a] Several independent experiments yield a factor of 4 ± 1 for different abundances of $CO_2^{-\cdot}$ for precursor ions formed via EI and CI, respectively.

$$CO_2^{+\cdot} + 2e^- \rightarrow O^{-\cdot} + CO \quad (6)$$

In addition, traces of $O_2^{-\cdot}$ and of $C^{-\cdot}$ fragments are observed in the $^{+}CR^{-}$ spectrum; the absence of any other signals excludes the presence of isobaric interferences in the precursor ion beam. Interestingly, the abundance of the $CO_2^{-\cdot}$ signal *decreases* by a factor of about 4 ± 1 when changing the ionization conditions from EI to CI by reducing the repeller voltage in the ion source while all other focusing conditions are kept constant. In general, the internal energy content of the precursor ions is much smaller in CI than under EI conditions, and thus changing the ionization conditions can be used to alter the population of ground and excited states in the $CO_2^{+\cdot}$ ions formed [42]. In particular, self-CI of carbon dioxide allows for electron transfer from neutral CO_2 to the initially formed molecular ions such that the average internal energy is likely to be close to the temperature of the ion source (200 °C). Accordingly, we arrive at the surprising conclusion that an increase of the internal energy of the precursor cation is associated with an increase of the yield for metastable $CO_2^{-\cdot}$ anion radical. In addition, we have determined the energy deficit (ΔE_{CR}) associated with charge reversal according to reaction (7).

$$CO_2^{+\cdot} + 2Xe \rightarrow CO_2^{-\cdot} + 2Xe^{+\cdot} \quad (7)$$

Experimentally, a value of $\Delta E_{CR} = 10.6 \pm 0.6$ eV is found. ΔE_{CR} depends on the vertical recombination energy of the $CO_2^{+\cdot}$ cation which is approximated by the ionization energy of neutral CO_2 because the neutral and cation structures are rather similar (see below), the ionization energy of xenon which is used as a target gas, and the electron affinity of CO_2 (see below). To a first approximation, we may thus assume $\Delta E_{CR} = 2\,IE(Xe) - IE(CO_2) - EA(CO_2)$. Using IE(Xe) = 12.1 eV and IE(CO_2) = 13.8 eV, we arrive at an estimate of EA(CO_2) = −0.2 ± 0.6 eV. Although the experimental error on this figure is sizable, the magnitude of the ΔE_{CR} rules out the formation of highly excited states or high-energy isomers of $[C,O_2]^{-\cdot}$.

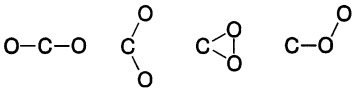

Scheme 1.

Finally, an estimate of the lower bound of the lifetime of metastable $CO_2^{-\cdot}$ anion radical was obtained by producing it via collisional activation of $HCOO^-$ in the field-free region between *B*(1) and *E*(1) and transmitting the $CO_2^{-\cdot}$ fragment through the remaining sectors *E*(1), *B*(2), and *E*(2), respectively. Within experimental error (±20%), no significant decrease of the $CO_2^{-\cdot}$ signal relative to the transmission of the $HCOO^-$ precursor was found. Accordingly, the lifetime of the metastable anion radical must exceed 50 μs, and this lower bound is well consistent with a value of 90 ± 20 μs reported previously [3,20].

3.2. Theoretical results

Four fundamentally different structures are conceivable for an anion radical $[C,O_2]^{-\cdot}$ (Scheme 1, Table 3): (i) linear carbon dioxide, **I**, (ii) a similar, but bent configuration, **II**, (iii) the dioxiranylidene structure **III**, and (iv) a peroxymethine species **IV**. Note that despite several proposals [9,10,38] an ion-dipole type complex $[O^{-\cdot} \cdot CO]$ could not be located as a minimum; instead upon geometry optimization such structures collapse to **I** and/or **II**. In line with previous theoretical studies at the *G*2 level of theory [43], the possible dioxirane isomer **III** indeed has a significant positive electron affinity with respect to the corresponding neutral, but both the anion and the neutral represent high-energy isomers are situated well above

Table 3
Calculated total (in Hartree)[a] and relative energies (in kcal/mol),[b] bond lengths (in Å), angles (in degree), and vibrational frequencies (in cm^{-1})[c] of the minima found for neutral $[C,O_2]$ and anionic $[C,O_2]^{-\cdot}$ at the B3LYP/6-311++G(d,p) level of theory.

Species	E_{total}	E_{rel}	r_{C-O}	α_{OCO}	$\nu_{sym\ stretch}$	$\nu_{asym\ stretch}$	$\nu_{bending}$
OCO, **I**	−188.635227	0.0	1.161	180.0	2324	1318	642
$OCO^{-\cdot}$, $\mathbf{II}^{-\cdot}$	−188.624879	6.5	1.231	137.8	650	1690	1172
$c-CO_2^{-\cdot}$, $\mathbf{III}^{-\cdot}$	−188.539436	60.1	1.306	100.6	1290	855	660[d]
$c-CO_2^{-\cdot}$, $\mathbf{III}^{-\cdot}$	−188.406143	143.8	1.446	62.3	1071	468	787[d]
$c-CO_2$, **III**	−188.402756	145.9	1.321	71.4	1421	587	799[d]
COO, **IV**	−188.368434	167.4	1.140[e]	180.0[e]	1988[e]	862[e]	199[e]

[a] Calculated total energies including ZPVE (unscaled).
[b] Energies relative to the $CO_2 + e^-$ asymptote.
[c] Harmonic frequencies scaled by 0.96.
[d] This mode is doubly degenerate.
[e] For the sake of simplicity, we included the coordinates of **IV** in this Table. There exists an additional bond length (r_{C-O} = 1.298 Å), and, of course, for isomer **IV** the angle refers to α_{COO} instead of α_{OCO} and the frequencies denote ν_{CO}, ν_{OO}, and $\nu_{bending}$, respectively.

the asymptote for $CO_2 + e^-$. The peroxy isomer **IV** could be located as a shallow minimum on the neutral surface, while all attempts failed to localize structure **IV** as a minimum on the anion-radical surface. Therefore, with regard to the energy deficit measured in the $^+CR^-$ experiments, the high-energy isomers **III** and **IV** cannot account for the anion signal, and we must focus on the low-energy part of the $[C,O_2]^{-\cdot}$ potential-energy surface with paying particular attention to electron detachment [20,21].

Fig. 1 slices through the potential-energy surfaces for $CO_2^{-\cdot}$ and CO_2 obtained at the BECKE3LYP/6-311++G(d,p) level of theory together with single-point energies obtained at the CCSD(*T*)/aug-cc-p-

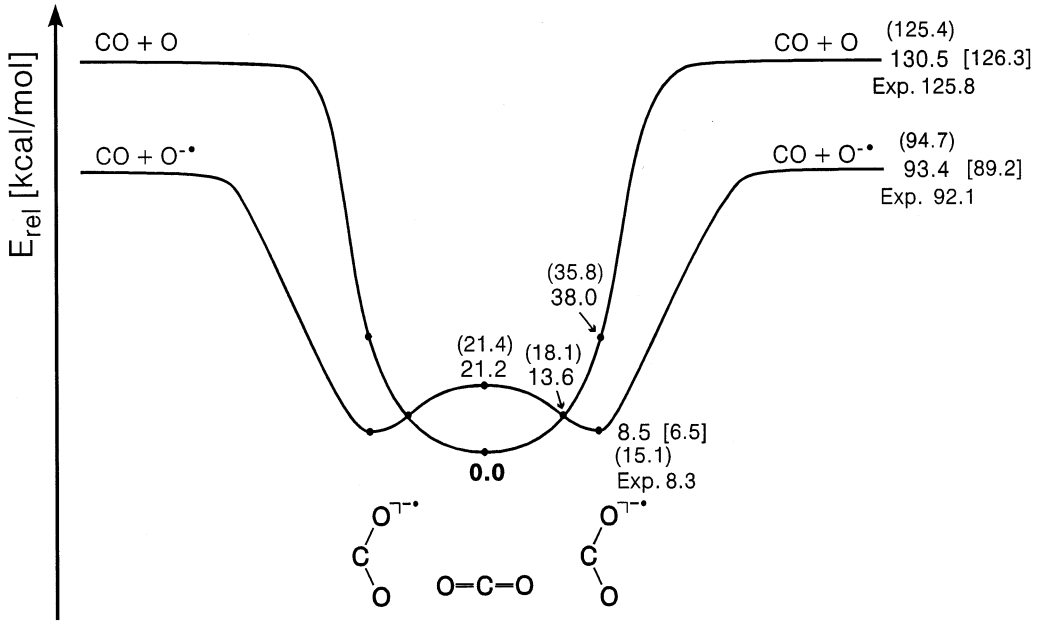

Fig. 1. Schematic presentation of the energetics of CO_2, $CO_2^{-\cdot}$, and the CO + O (^3P) fragmentation channel at the BECKE3LYP/6-311++G(d,p) level of theory. Numbers in brackets include zero-point energy corrections and the figures in square brackets refer to the CCSD(*T*)/aug-cc-pVTZ//BECKE3LYP/6-311++G(d,p) calculations. Experimental data are given for comparison, note that the dissociation of neutral CO_2 to yield CO + O (^3P) is a spin-forbidden process.

Table 4
Calculated energetics (in kcal/mol),[a] bond lengths (in Å) and angles (in degree) of $CO_2^{+/0/-}$ and the MECP between the neutral and anion surface as well as the vibrational frequencies of the minima (in cm^{-1})[b] obtained at the B3LYP/6-311++G(d,p) and CCSD(*T*)/aug-cc-pVTZ levels of theory.

Species	$E_{CCSD(T)}$[c]	E_{B3LYP}	r_{C-O}	α_{OCO}	$\nu_{asym\ stretch}$	$\nu_{sym\ stretch}$	$\nu_{bending}$
CO_2	0.0	0.0	1.161	180.0	2324	1318	642[d]
MECP *A*[e,f]	—[g]	13.7	1.193	153.6			
MECP *B*[e,f]	18.1	—[g]	1.203	149.1			
$CO_2^{-\cdot}$	15.1	8.5	1.231	137.8	1690	1172	650[d]
$CO_2^{-\cdot}$[h]	21.4	21.2	1.161	180.0			
CO_2[i]	35.8	37.9	1.231	137.8			
$CO_2^{+\cdot}$	—[j]	317.8	1.171	180.0	1435	1262	550/452[k]

[a] Calculated energies relative to the $CO_2 + e^-$ asymptote; for the effect of the ZPVE corrections, see text.
[b] Harmonic B3LYP/6-311++G(d,p) frequencies scaled by a factor of 0.96.
[c] Single-point energies using the geometries obtained with B3LYP/6-311++G(d,p).
[d] This mode is doubly degenerate.
[e] The MECPs *A* and *B* were located at the B3LYP/6-311++G(d,p) and CCSD(*T*)/aug-cc-pVTZ//B3LYP/6-311++G(d,p) levels of theory, using the method described in [37].
[f] No frequencies available.
[g] Not defined.
[h] Energy of the anion radical with the geometry of linear, neutral CO_2; frequencies are not defined for this point.
[i] Energy of neutral CO_2 with the geometry of the anion radical; frequencies are not defined for this point.
[j] Not calculated.
[k] Due to program limitations, the full symmetry of the corresponding π state cannot be represented, the resulting symmetry breaking explains why B3LYP/6-311++G(d,p) predicts two non equal instead of one, doubly degenerate frequency for the bending mode.

VTZ level. While BECKE3LYP and CCSD(*T*) show some quantitative divergence, the overall pictures are similar. Thus, the linear ground state of neutral carbon dioxide **I** has a negative vertical electron affinity (EA_v) of about −1 eV, but the bent geometry **II** has a positive EA_v. The adiabatic EA is calculated as $EA_a(CO_2)$ = −0.37 eV and −0.65 eV with BECKE3LYP and CCSD(*T*), respectively. Note that similar values, i.e. $EA_a(CO_2)$ = −0.53 eV and −0.67 eV, have recently been obtained with BECKE3LYP and CCSD(*T*), respectively, using the 6-311+G(3df) basis set [21]. Inclusion of zero-point vibrational energy slightly stabilizes the anion by about 0.1 eV relative to neutral CO_2, but the metastability of the anion radical with respect to electron detachment is beyond any doubt. The theoretically predicted $EA_a(CO_2)$ agrees well with the results of other previous high-level calculations, i.e. ca. −0.75 eV [8] and −0.62 eV [19], as well as the experimental value of −0.6 ± 0.2 eV obtained by Compton et al. [3].

Along with the bending of the anion radical, electron transfer to carbon dioxide weakens the stretching frequencies considerably (Table 4) such that chemical activation of carbon dioxide should become more facile than in the neutral species. Due to the sizable negative EA_v of the neutral, the minimal energy crossing point (MECP) of the anionic and neutral surfaces is in the vicinity of the anion geometry. The MECP is crucial for the stability of the metastable anion radical because the intersection of both curves indicates the region in which spontaneous electron detachment from vibrational hot $CO_2^{-\cdot}$ can occur, while at sufficiently low internal energies, the bent species **II** is trapped within the potential well of the O–C–O bending mode. A few vibrational modes fit into this barrier height and thus theory predicts that metastable $CO_2^{-\cdot}$ exists as a long-lived species. Also, the theoretical results imply that the anion radical can be formed from appropriate precursors in which the O–C–O unit is bent.

As far as charge inversion of $CO_2^{+\cdot}$ is concerned, theory predicts that the geometries of the neutral and the cation are very similar (Table 4), i.e. the vertical recombination energy for the process $CO_2^{+\cdot} + e^- \rightarrow CO_2$ differs only by about 0.01 eV from the adiabatic IE of CO_2. Further, as outlined above, an electron

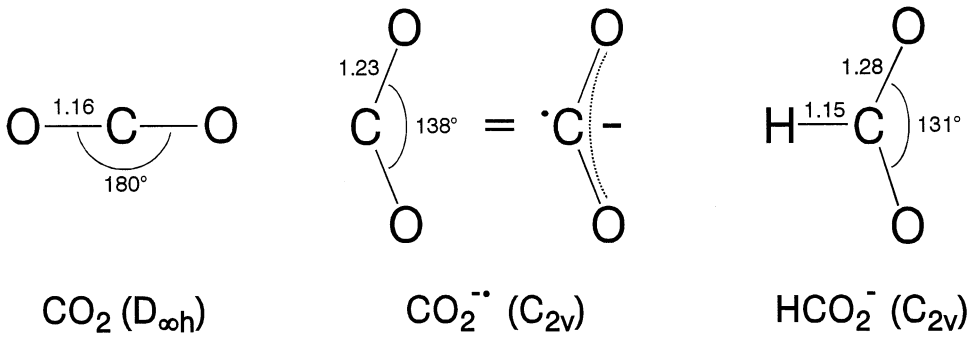

Fig. 2. Geometries of neutral CO_2, the $CO_2^{-\cdot}$ anion radical, and formate ion HCO_2^- calculated at the BECKE3LYP/6-311++G(d,p) level of theory (bond lengths in Å, angles in degrees).

cannot be attached to the linear form of neutral CO_2 to yield a stable anion radical. What matters therefore is the internal energy content of the neutral species which determines the propensity of CO_2 molecules with sufficiently bent geometries due to vibrational excitation. The energies required to excite the corresponding degenerate bending modes are relatively low in both the cationic and the neutral forms of CO_2 (Table 4). For example, the calculated bending frequency of 642 cm^{-1} for neutral CO_2 corresponds to a vibrational temperature of about 900 K, such that at the ion source temperature of about 473 K a significant fraction of the neutrals can populate vibronic levels other than $v = 0$ [44].

4. Discussion

Although a further mass spectrometric characterization of the $[C,O_2]^{-\cdot}$ ion was impossible due to very low ion yields, both the choice of the precursors and the internally consistent results exclude that isobaric interferences give rise to the signal observed at $m/z = 44$ amu. Further, the energy deficit measured for charge inversion of $CO_2^{+\cdot}$ rules out the high-energy isomers **III** and **IV** as candidates to explain the $[C,O_2]^{-\cdot}$ signal, because these would be associated with significantly different values for ΔE_{CR} (see above). However, the possible formation of minute amounts of these peroxy isomers is indicated by the observation of a very weak, but yet distinct signal for $O_2^{-\cdot}$ in the $^+CR^-$ spectrum of $CO_2^{+\cdot}$. Notwithstanding, the very low abundance of this fragment cannot be taken as direct evidence for the formation of isomers **III** or **IV** because O–O bond formation concomitant with loss of a carbon atom may also occur en route to the dissociation of energized $CO_2^{+/0/-}$ without involving structures **III** or **IV** as discrete minima.

In summary, the experimental findings are compatible with the formation of the metastable $CO_2^{-\cdot}$ anion radical with a bent geometry. For this species, theory predicts a $^2A_1$ state in which the unpaired electron resides in a σ-type orbital at the carbon center. Accordingly, $CO_2^{-\cdot}$ ($^2A_1$) can schematically be described as carbon dioxide in which one C–O double bond is broken by electron attachment to yield a carbon centered radical together with a delocalized carboxylate type anion (Fig. 2). This bonding situation corresponds to a separation of charge and radical centers which is typical for distonic ions [46,47]. In contrast to most known distonic ions, however, in $CO_2^{-\cdot}$ ($^2A_1$) this separation is not afforded by spacing atoms or groups but rather is due to the fact that the negative charge and the uncoupled electron reside in different planes (σ and π) of the molecule. Along with this reasoning, the C–O stretching frequencies decrease significantly from the neutral to the anion radical. Strong support for the formation of metastable $CO_2^{-\cdot}$ is also provided by the charge-reversal experiments performed at different ionization conditions. Conceptually, electron ionization leads to more excitation and thus a higher internal energy of the $CO_2^{+\cdot}$ precursor ions than does chemical ionization.

As a consequence, the population of bent geometries in the precursor beam is higher in EI than in CI. This conjecture can account for the seemingly puzzling finding that the yield of $CO_2^{-\cdot}$, i.e. a metastable anion trapped in a rather shallow potential-energy well, increases with the internal energy content of the precursor. Though we cannot specify the variation of the internal energy when switching form EI to CI, the qualitative result is in accord with the formation of genuine $CO_2^{-\cdot}$.

While these experimental findings are fully in line with the theoretical predictions, the formation of $CO_2^{-\cdot}$ upon collisional activation of formate ion [11,38] becomes even more intriguing. Though we may assume that carboxylates may serve as suitable precursors for the formation of $CO_2^{-\cdot}$ due to the preformed bent O–C–O moiety, even the vertical electron affinity of bent CO_2 is so low that rapid electron transfer to the departing radical should predominate for R = H due to the sizable EA of the hydrogen atom (0.78 eV). Moreover, the formation of $CO_2^{-\cdot}$ with a μs lifetime would indicate that the shallow potential energy well of the anion radical is directly accessed in a high-energy collision; however, this is in conflict with the apparent kinetic energy release of about 200 meV which is associated with loss of a H atom from $HCOO^-$. These considerations do not agree with simple homolytic C–H bond cleavage upon collisional activation [16,47,48]. Instead, we propose that $CO_2^{-\cdot}$ is generated from formate ion in a multicollision process following the sequence depicted in reactions (8)–(10).

$$HCOO^- \rightarrow HCOO^{\cdot} + e^- \quad (8)$$

$$HCOO^{\cdot} \rightarrow H^{\cdot} + CO_2 \quad (9)$$

$$CO_2 + Xe \rightarrow CO_2^{-\cdot} + Xe^{+\cdot} \quad (10)$$

In the first step, collisional electron detachment gives rise to formoxy radical. Either in a second collision or due to the internal energy deposited in the neutral in the first collision, the neutral radical subsequently dissociates to afford neutral carbon dioxide [40,41]. This neutral may still contain a substantial amount of internal energy and its bent forms may then be re-ionized in another collision with the target gas to give rise to the observed $CO_2^{-\cdot}$ signal. This scenario accounts for both the peak width as a result of multiple collisional broadening, and the target gas effect, because collisional electron transfer from a target gas to a fast moving neutral is much more facile for xenon (IE = 12.1 eV) than for helium (IE = 24.5 eV). In conclusion, it is suggested that metastable $CO_2^{-\cdot}$ is not formed by simple dissociation of collisionally activated formate ion, but originates from two sequential electron transfer events in which the carboxylate just serves as a precursor to generate a beam of fast-moving neutral CO_2 with a significant population of bent geometries. In marked contrast, the collisional activation of higher carboxylates, e.g. i-$C_3H_7COO^-$ [13], can proceed via reaction (4), because (i) the homolytic bond cleavage becomes more facile if a secondary radical is formed and (ii) the isopropyl radical has a negative electron affinity [15,16,48].

Finally, we would like to mention some notable differences in the calculations of the MECP for the neutral and anion surfaces with BECKE3LYP and CCSD(T), respectively. While the potential-energy curves for neutral CO_2 are quite similar, the anion minimum is more pronounced with BECKE3LYP than with CCSD(T). As a consequence, the crossing of the surfaces occurs at a higher energy relative to the minimum at the BECKE3LYP level, giving an increased height of the resulting effective barrier for electron detachment. The coupled-cluster calculations, using quite large basis sets, should give a more reliable picture of the relative energies of the two surfaces, in which there is a real, but rather small "barrier" to electron loss [21]. This accounts for the lower bracket of 50 μs for the anion's lifetime, but also suggests that the real value may not be substantially higher; in complete agreement with the previously estimated lifetime of about 90 μs [3,20].

5. Conclusion

The anion radical of carbon dioxide can be made by electron transfer to neutral CO_2 in high-energy

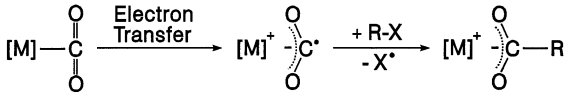

Scheme 2.

collisions as well as by collisional activation of some carboxylate ions. Although $CO_2^{-\cdot}$ is metastable with respect to electron detachment, the OCO bending potential provides a significant barrier so that in the gas phase the anion radical of carbon dioxide exhibits a lifetime in the upper microsecond regime. Further, rovibrational excitation of the precursor ions represents a clue to increase the yield of the metastable $CO_2^{-\cdot}$ anion radical in charge-reversal experiments; thus, in these experiments "hot" ions can lead to "cold" neutrals due to favorable Franck-Condon factors for the excited species. In particular, the present results provide yet another demonstration of the intuitively surprising fact that high-energy collisions can be used to probe rather shallow minima with well depths of a few kcal/mol in charge-transfer experiments [12,27,49].

The fact that the bonding situation in $CO_2^{-\cdot}$ can be described in terms of a carboxylate anion with distinct radical character at the carbon center proposes a route for the activation of carbon dioxide by a sequence of electron transfer and radical-type reactions. While neither direct electron transfer nor radical attachment to neutral carbon dioxide appear as feasible routes, both processes may become more facile in the presence of transition metal complexes [*M*] as shown in Scheme 2 [1].

Thus, complexation of CO_2 by a neutral transition-metal fragment may induce some distortion of the carbon dioxide moiety and by such increase its electron affinity [2]. Furthermore, the product formed by electron transfer may experience electrostatic stabilization by the bonding between the positively charged metal fragment and the carboxylate residue and by such render the formation of a carbon centered radical more likely which may then react with appropriate reagents *R-X* with sufficiently weak covalent bonds (e.g. alkyl iodides, disulfides) or with other sources of radicals.

Acknowledgements

We thank the Volkswagen-Stiftung, the Deutsche Forschungsgemeinschaft, and the Fonds der Chemischen Industrie for financial support. Professor K.H. Bowen is appreciated for sending us reprints with photodetachment spectra of $(CO_2)_n^{-\cdot}$ ions. We thank Dr. C. Heinemann and Dr. M.C. Holthausen for the permission to quote some results of their unpublished work on high-energy isomers of carbon dioxide [44]. Further, we appreciate inspiring comments by Professor H. Zipse on this topic.

References

[1] A. Behr, Carbon Dioxide Activation by Metal Compounds, VCH, Weinheim, 1988.
[2] E. Fujita, L.R. Furenlid, M.W. Renner, J. Am. Chem. Soc. 119 (1997) 4549.
[3] R.N. Compton, P.W. Reinhardt, C.D. Cooper, J. Chem. Phys. 63 (1975) 3821.
[4] For an overview, see: T. Tsukuda, M.A. Johnson, T. Nagata, Chem. Phys. Lett. 268 (1997) 429.
[5] R.A. Holroyd, K. Itoh, M. Nishikawa, Chem. Phys. Lett. 266 (1997) 227.
[6] K.O. Hartman, I.C. Hisatsune, J. Chem. Phys. 44 (1966) 1913.
[7] K.H. Bowen, J.G. Eaton, in The Structure of Small Molecules and Ions, R. Naaman and Z. Vager (Eds.), Plenum, New York, 1988, p. 147.
[8] L.B. Knight Jr., D. Hill, K. Berry, R. Babb, D. Feller, J. Chem. Phys. 105 (1996) 5672.
[9] J.M. Van Doren, S.E. Barlow, C.H. DePuy, V.M. Bierbaum, J. Am. Chem. Soc. 109 (1987) 4412.
[10] J.M. Van Doren, S.E. Barlow, C.H. DePuy, V.M. Bierbaum, Int. J. Mass Spectrom. Ion Processes 109 (1991) 305.
[11] C.A. Schalley, D. Schröder, H. Schwarz, K. Möbus, G. Boche, Chem. Ber./Recueil, 130 (1997) 1085.
[12] C.A. Schalley, Dissertation, Technische Universität Berlin D83, Gas-Phase Ion Chemistry of Peroxides, Shaker Verlag, Herzogenrath, Germany, 1997.
[13] D. Schröder, N. Goldberg, W. Zummack, H. Schwarz, J.C. Poutsma, R.R. Squires, Int. J. Mass Spectrom. Ion Processes 165/166 (1997) 71.
[14] M.B. Stringer, J.H. Bowie, P.C.H. Eichinger, G.J. Currie, J. Chem. Soc. Perkin Trans. 2 (1987) 385.
[15] S.T. Graul, R.R. Squires, J. Am. Chem. Soc. 110 (1988) 607.
[16] S.T. Graul, R.R. Squires, J. Am. Chem. Soc. 112 (1990) 2506 and 2517.
[17] J. Pacansky, U. Wahlgren, P.S. Bagus, J. Chem. Phys. 72 (1975) 2740.
[18] D.G. Hopper, Chem. Phys. 53 (1980) 85.

[19] D. Yu, A. Rauk, D.A. Armstrong, J. Phys. Chem. 96 (1992) 6031.
[20] A. Rauk, D.A. Armstrong, D. Yu, Int. J. Chem. Kinet. 26 (194) 7.
[21] G.L. Gutsev, R.J. Bartlett, R.N. Compton, J. Chem. Phys. 108 (1998) 6756.
[22] R. Srinivas, D. Sülze, T. Weiske, H. Schwarz, Int. J. Mass Spectrom. Ion Processes 107 (1991) 368.
[23] C.A. Schalley, D. Schröder, H. Schwarz, Int. J. Mass Spectrom. Ion Processes 153 (1996) 173.
[24] M.M. Bursey, Mass Spectrom. Rev. 9 (1990) 555.
[25] If not mentioned otherwise, thermochemical data have been taken from: S.G. Lias, J.E. Bartmess, J.F. Liebman, J.L. Holmes, R.D. Levin, W.G. Mallard, J. Phys. Chem. Ref. Data 17 (1998), Suppl. 1.
[26] J.N. Harvey, C. Heinemann, A. Fiedler, D. Schröder, H. Schwarz, Chem. Eur. J. 2 (1996) 1230.
[27] D. Schröder, C.A. Schalley, J. Hrušák, N. Goldberg, H. Schwarz, Chem. Eur. J. 2 (1996) 1235.
[28] J.N. Harvey, D. Schröder, H. Schwarz, Bull. Soc. Chim. Belg. 106 (1997) 447.
[29] GAUSSIAN 94, Revision B3, M.J. Frisch, G.W. Trucks, H.B. Schlegel, P.M.W. Gill, B.G. Johnson, M.A. Robb, J.R. Cheeseman, T. Keith, G.A. Petersson, J.A. Montgomery, K. Raghavachari, M.A. Al-Laham, V.G. Zakrzewski, J.V. Ortiz, J.B. Foresman, C.Y. Peng, P.Y. Ayala, W. Chen, M.W. Wong, J.L. Anders, E.S. Replogle, R. Gomperts, R.L. Martin, D.J. Fox, J.S. Binkley, D.J. Defrees, J. Baker, J.J.P. Stewart, M. Head-Gordon, C. Gonzalez, J.A. Pople, GAUSSIAN Inc., Pittsburgh, PA, 1995.
[30] P.J. Knowles, C. Hampel, H.-J. Werner, J. Chem. Phys. 99 (1993) 5219.
[31] MOLPRO 96.4 is a package of ab initio programs written by H.-J. Werner and P.J. Knowles with contributions from: J. Almlöf, R.D. Amos, M.J.O. Deegan, S.T. Elbert, C. Hampel, W. Meyer, K. Peterson, R. Pitzer, A.J. Stone, P.R. Taylor and R. Lindh.
[32] T.H. Dunning Jr., J. Chem. Phys. 90 (1989) 1007.
[33] R.A. Kendall, T.H. Dunning Jr., R.J. Harrison, J. Chem. Phys. 96 (1992) 6796.
[34] N. Koga, K. Morokuma, Chem. Phys. Lett. 119 (1985) 371.
[35] D.R. Yarkony, J. Phys. Chem. 97 (1993) 4407.
[36] M. Bearpark, M.A. Robb, H.B. Schlegel, Chem. Phys. Lett. 223 (1994) 269.
[37] J.N. Harvey, M. Aschi, H. Schwarz, W. Koch, Theor. Chem. Acc. 99 (1998) 95.
[38] J.C. Sheldon, J.H. Bowie, J. Am. Chem. Soc. 112 (1990) 2424.
[39] C.A. Schalley, G. Hornung, D. Schröder, H. Schwarz, J. Chem. Soc. Rev. 27 (1998) 91.
[40] C.A. Schalley, G. Hornung, D. Schröder, H. Schwarz, Int. J. Mass Spectrom. Ion Processes 172/173 (1998) 181.
[41] For a real-time observation of carbon–carbon bond scission in carboxylates upon photoinduced electron transfer, see: T.M. Bockman, S.M. Hubig, J.K. Kochi, J. Am. Chem. Soc. 118 (1996) 4502.
[42] C. Heinemann, D. Schröder, H. Schwarz, J. Phys. Chem. 99 (1995) 16195.
[43] C. Heinemann and M.C. Holthausen, unpublished results.
[44] For the UV absorption spectrum of hot CO_2, see: R.J. Jensen, R.D. Guettler, J.L. Lyman, Chem. Phys. Lett. 277 (1997) 356.
[45] B.F. Yates, W.J. Bouma, L. Radom, J. Am. Chem. Soc. 106 (1984) 5805.
[46] K.M. Stirk, L.K.M. Kiminkinen, H.I. Kenttämaa, Acc. Chem. Res. 92 (1992) 1649.
[47] S.T. Graul, Ph.D. Thesis, Purdue University, 1989.
[48] C.H. DePuy, S. Gronert, S.E. Barlow, V.M. Bierbaum, R. Damrauer, J. Am. Chem. Soc. 111 (1989) 1968.
[49] D. Schröder, J.N. Harvey, M. Aschi, H. Schwarz, J. Chem. Phys. 108 (1998) 8446.